GEOPHYSICS, VOL. 69, NO. 6 (NOVEMBER-DECEMBER 2004); P. 1521–1529, 7 FIGS., 2 TABLES.
10.1190/1.1836825

Improving *Q* estimates from seismic reflection data using well-log-based localized spectral correction

Chris L. Hackert[1] and Jorge O. Parra[1]

ABSTRACT

Most methods for deriving *Q* from surface-seismic data depend on the spectral content of the reflection. The spectrum of the reflected wave may be affected by the presence of thin beds in the formation, which makes *Q* estimates less reliable. We incorporate a method for correcting the reflected spectrum to remove local thin-bed effects into the *Q*-versus-offset (QVO) method for determining attenuation from seismic-reflection data. By dividing the observed spectrum by the local spectrum of the known reflectivity sequence from a nearby well log, we obtain a spectrum more closely resembling that which would be produced by a single primary reflector. This operation, equivalent to deconvolution in the time domain, is demonstrated to be successful using synthetic data. As a test case, we also apply the correction method to QVO with a real seismic line over a south Florida site containing many thin sandstone and carbonate beds. When corrected spectra are used, there is significantly less variance in the estimated *Q* values, and fewer unphysical negative *Q* values are obtained. Based on this method, it appears that sediments at the Florida site have a *Q* near 33 that is roughly constant from 170- to 600-m depth over the length of the line.

INTRODUCTION

As seismic analysis becomes more advanced, interpreters now examine the smallest details of the seismic records. In the effort to extract more and more useful information from seismic data, geophysicists have developed techniques to look not only at the sequence of reflections, but also bright spots, amplitude variation with offset and azimuth (AVO/AVA), and even instantaneous attributes such as frequency and phase. It seems likely that knowledge of *Q*, the quality factor of the medium, will one day be important for providing additional information about the formation. In addition to the well-known features of gas and fractures being associated with low *Q* (high attenuation of seismic waves), a number of recent works have proposed using *Q* as an indicator of reservoir quality (Parra and Hackert, 2002; Pride et al., 2003; Rapoport et al., 2004; Korneev et al., 2004) and using *Q* as a numerical basis for "inverse filtering" (Zhang and Ulrych, 2002). Inverse filtering involves raising the high-frequency content of later times in seismic sections to compensate for attenuation of the seismic wave and improve the resolution of the image.

Several projects have demonstrated the calculation of *Q* from seismic transmission data, such as VSP (e.g., Hauge, 1981), crosswell (e.g., Quan and Harris, 1995; Neep et al., 1996) and sonic logging (e.g., Sun et al., 2000). Very few publications, however, have addressed computing *Q* from reflection data, and even fewer have published *Q*-value estimates from real surface seismic data. Dasgupta and Clark (1998) is a notable exception. Part of the reason for this is the complexity of surface seismic data. Compared to transmission signals, reflection signals have a longer path length since they must travel back to the surface. The amplitude is further reduced by the reflection coefficient of the layer of interest (usually less than 0.1). A single stacked common-depth-point (CDP) reflection event is also comprised of signals from multiple offsets, each representing a different travel path, path length, angle of incidence, and source-receiver pair. Nevertheless, surface seismic data is so useful and common that it is worthwhile to attempt to recover *Q* values from this source.

In reflection data, *Q* must be computed from the change in spectra of the reflections. As a seismic wave travels through an attenuating medium, the high frequencies are attenuated more quickly than the lower frequencies. (We will assume that *Q* in the rock is constant over the bandwidth of the source.) Two primary methods have been proposed for computing *Q* from changes in a signal's spectral characteristics: the log-spectral-ratio (LSR) method, which calculates the reduction in amplitude of each frequency in the spectrum; and the frequency-shift method, which calculates the shift in the peak or centroid of the spectrum (e.g., Quan and Harris, 1995; Zhang and Ulrych,

Manuscript received by the Editor November 10, 2003; revised manuscript received May 20, 2004.
[1]Southwest Research Institute, Applied Physics Division, 6220 Culebra Road, San Antonio, Texas 78238. E-mail: chackert@swri.org; jparra@swri.edu.

2002). Both methods assume that attenuation is the only thing that affects the shape of the reflection spectra.

In fact, in many sedimentary formations, the reflection spectra have a significant component from interfering, closely spaced reflections. This gives rise to the well-known tuning effect (e.g., Sheriff and Geldart, 1995), in which amplitudes may be increased or decreased by constructive or destructive interference from reflectors less than a quarter-wavelength apart. In addition to the amplitude changes, however, there is also a change in the apparent frequency and phase of the reflected wave, as noted by Robertson and Nogami (1984), as well as Raikes and White (1984). In this paper, we examine how the changes in the apparent frequency caused by thin beds affect the spectrum of the reflected wave and, in turn, affect the computation of Q from seismic reflection data. We are not concerned with analyzing or interpreting the absorption caused by short period multiples (e.g., O'Doherty and Anstey, 1971) but rather with correcting for the influence of local thin-bed primaries on the windowed reflection spectrum. We combine a method for using well-log data to correct for the thin-bed effect (Raikes and White, 1984) with the Q-versus-offset (QVO) method of Dasgupta and Clark (1998) and demonstrate its successful application in computing Q from both synthetic and real surface seismic data.

METHOD

Our method for computing Q as a function of CDP is the Q-versus-offset (QVO) method, as described by Dasgupta and Clark (1998), although we employ both the LSR method and the centroid frequency-shift method (CF) as described in Quan and Harris (1995) to evaluate the spectral changes. The peak-frequency shift method, applied to surface seismic data in Zhang and Ulrych (2002), was also tried but was found to be too sensitive to noise and other perturbations to the spectrum. Both the LSR and CF methods depend on comparing the spectrum of the target signal with a reference spectrum. The reference spectrum is ideally that of the source; but since that is often unavailable, a shallow strong reflection may be substituted. Briefly, the QVO calculation involves taking post-normal moveout (NMO) CDP gathers, stacking several adjacent offsets within each CDP gather to improve the signal-to-noise ratio, computing Q for each offset stack within each CDP (using LSR and/or CF), and extrapolating the resulting Q values to zero offset for each CDP using a least-squares fit. The resulting Q indicates the attenuation between the reference reflector and the target reflector.

One difficulty with computing Q from surface seismic data is that both the LSR and CF methods for determining Q were originally derived for use with transmission data rather than reflection data. The recorded signal in a transmission experiment is the directly transmitted pulse plus a coda of forward-scattered energy. Since the coda is necessarily delayed with respect to the directly transmitted wave, the two may be at least partially separated with time gating. This results in a relatively robust estimate of the transmitted pulse spectrum. Ganley and Kanasewich (1980) examined how thin-bed multiples affect the LSR method for transmitted waves and proposed a correction based on synthetic seismograms.

In reflection data, the reflected wave train is the convolution in the time domain of the apparent source wavelet with the reflection spike-time series "stickogram" (Sheriff and Geldart, 1995). Since convolution in the time domain is equivalent to multiplication in the frequency domain (Oppenheim and Schafer, 1989), the spectrum of the reflected pulse can be distorted by closely spaced reflectors. Figure 1 demonstrates this effect. For a single isolated reflector (Figure 1a), no spectral distortion is seen. For the three evenly spaced reflectors shown in Figure 1b (with the same total reflectivity as Figure 1a), the spectrum of the reflected wave will be enhanced near 50 Hz and suppressed near 20 and 80 Hz. This effect arises from constructive and destructive interference of the reflections at certain frequencies. Finally, if there are many closely but randomly spaced reflectors (as in Figure 1c), the reflected spectrum may be affected irregularly. It could suppress low-frequency content in the combined reflection, as in this case, which will give the appearance of negative Q through increased amplitude at high frequencies.

Raikes and White (1984) and White (1992) discuss a method for correcting for these effects, which we will outline here. Consider a source pulse $s(t)$ with corresponding spectrum $S(\omega)$. (We will use a convention of lower-case letters denoting time-domain data and upper-case letters denoting the equivalent frequency-domain data.) The source pulse travels through a layered earth, for which the reflectivity stickogram $r(t)$ is the reflection coefficient at two-way traveltime t, and $g(t)$ describes the geometric spreading loss in amplitude. If the layered medium is elastic, the resulting observed (primaries-only) reflected signal, $a(t)$, is given by

$$a(t) = g(t) \int_{-\infty}^{\infty} s(\tau) r(t-\tau) d\tau. \tag{1}$$

In practice, the source pulse is finite, so only a small range of τ contributes to the integral. The convolution operation is linear time–invariant (Oppenheim and Schafer, 1989), so we may take a subset of reflectors, $r_1(t)$, which lie near two-way time t_1, and the local reflected wavetrain contribution from these reflectors will be

$$a_1(t) = g(t) \int_{-\infty}^{\infty} s(\tau) r_1(t-\tau) d\tau. \tag{2}$$

Then, the local spectrum of the reflected pulse near time t_1, $A_1(\omega)$, is approximately equal to

$$A_1(\omega) = g(t_1) S(\omega) R_1(\omega), \tag{3}$$

where $R_1(\omega)$ is the Fourier transform of $r_1(t)$.

If the layered medium is attenuating, with constant Q, then the spectrum will be reduced in a frequency-dependent manner such that

$$A_1(\omega) = g(t_1) S(\omega) R_1(\omega) \exp\left(-\frac{\omega t_1}{2Q}\right). \tag{4}$$

Similarly, the local subset of reflectors $r_2(t)$ near two-way time t_2 will generate a reflected pulse with spectrum $A_2(\omega)$. Taking the logarithm of the ratio of A_2 and A_1,

$$\ln\left(\frac{A_2(\omega)}{A_1(\omega)}\right) = \ln\left(\frac{g(t_2)}{g(t_1)}\right) + \ln\left(\frac{R_2(\omega)}{R_1(\omega)}\right) - \frac{\omega}{2Q}(t_2 - t_1). \tag{5}$$

The first term on the right-hand side is independent of frequency. If $R_1(\omega)$ and $R_2(\omega)$ are both independent of frequency [as they would be if $r_1(t)$ and $r_2(t)$ represent single, isolated

reflectors], then the second term on the right-hand side is also constant, and Q may be computed from the slope of the log-spectral ratio of A_2/A_1. This is exactly the traditional LSR method. If $r_1(t)$ or $r_2(t)$ represents a group of closely spaced reflectors, then the second term on the right-hand side will vary with frequency, and the slope of the LSR will not be directly proportional to $1/Q$.

When well-log impedance data is available, in principle we should be able to compute the $r(t)$ associated with a particular time window and hence derive the $R(\omega)$ that is needed to correct the spectral ratio. This should work at least for seismic traces near the well, where lateral variations in impedance or dipping beds will not have significantly altered the $r(t)$ profile. For such a case,

$$\ln\left(\frac{A_2(\omega)/R_2(\omega)}{A_1(\omega)/R_1(\omega)}\right) = \ln\left(\frac{g(t_2)}{g(t_1)}\right) - \frac{\omega}{2Q}(t_2 - t_1), \quad (6)$$

and we may again compute Q^{-1} from the slope of the known values on the left-hand side of the equation. Note that the $A(\omega)/R(\omega)$ is a local spectrum corrected for the primaries-only thin-bed effects and, as such, may also be used in frequency-shift methods for computing Q.

Given seismic data consisting of NMO-corrected CDP gathers processed without any kind of spectral balancing and a well log converted to reflectivity stickogram in two-way time, our method is

1) Select a reference reflection and one or more target reflections.

2) Apply a tapered time window such as the Hanning window (Oppenheim and Schafer, 1989) to each trace in the seismic data and the reflectivity stickogram. The time window should be short enough to select the reflection of interest but long enough that the frequency resolution (equal to the inverse of the time-window length) is sufficiently smaller than the bandwidth of the pulse. The tapered time window gradually reduces the influence of reflectors away from the two-way time of interest.

3) Take the Fourier transform of each time window, and divide the seismic spectrum amplitude by the amplitude of the reflectivity stickogram spectrum. We recommend smoothing the stickogram spectrum before the division, since it often contains zeros. These zeros result from assuming planar, laterally invariant reflectors and wave propagation at normal incidence. In reality, or even in multidimensional numerical simulation, these frequencies will correspond to spectral minima but not true zeros.

4) Using the local corrected spectra of the target and reference reflections, compute Q using the LSR and CF methods.

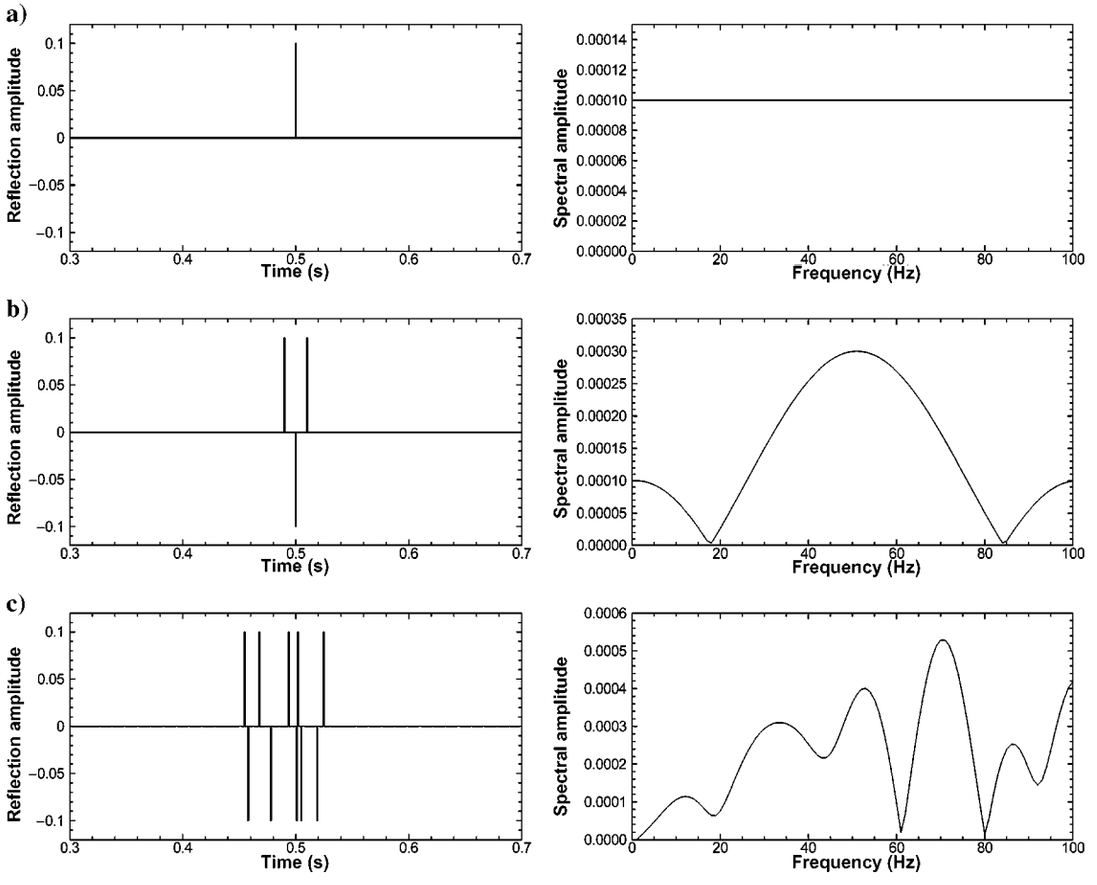

Figure 1. Three hypothetical spike reflectivity stickogram sequences and their corresponding spectra. The reflected pulse spectrum will be the product of the incident pulse spectrum and the spectrum of the spike sequence.

Following the QVO method of Dasgupta and Clark (1998), these values may be extrapolated to zero offset within each CDP, producing an average Q value for each CDP for each target reflection.

SYNTHETIC-DATA EXAMPLE

To test this method, we first used a synthetic-data example consisting of traces from a viscoelastic 2D finite-difference model. The model geometry consists of five layers (four reflectors), each with different Q and P-velocity (Figure 2). The model density and S-wave velocity are kept constant to eliminate any S-wave reflections that might interfere with the recorded signal. The 2D model consists of a staggered grid with normal stresses at cell centers, densities and displacements at cell faces, and shear stress at cell corners. The cells have 1-m spacing, and there are 2100 grid cells horizontally and 4500 grid cells vertically. The source pulse is a Ricker wavelet of 100-Hz peak frequency, and the time step is 0.25 ms. The absorbing boundary condition of Higdon (1991) is used to reduce reflections from the domain boundary, although the boundaries are placed sufficiently far from the source and receivers that no significant reflection would be detected. We use two variations on this model. In one case, there are no thin beds; in the second case, there are two thin beds added at each primary layer boundary, as shown in Figure 2.

Since there is no lateral variation in the model geometry, a single shot suffices to generate all necessary offsets. The resulting seismic data is shown for each case (processed with automatic gain control only) in Figure 3. We use the first reflection as the reference and compute the average Q between that and each later reflection using both the uncorrected and corrected spectra (Table 1). Based on this data, a layer-stripping method (Dasgupta and Clark, 1998) provides the Q of each individual layer as well. Time windows are 0.145 to 0.345 s for the first (reference) reflection, 0.528 to 0.908 s for the second reflection, 0.97 to 1.47 s for the third reflection, and 1.54 to 1.84 s for the fourth reflection. Only the LSR method is used in this synthetic example, because the large frequency shift between the first and fourth reflections invalidates some assumptions of the CF method. Since this is an almost ideal data set, it is not surprising that, with no thin beds present, the QVO method recovers the Q of each layer almost exactly. The thin beds at the layer boundaries of the second model, however, interfere with the reflection spectra in the manner discussed above, so that Q values of the uncorrected QVO method are quite poor. Applying the well-log–based spectral correction substantially removes this effect, and the corrected Q values are of reasonable accuracy.

The uncorrected and corrected normalized local spectra are shown in Figure 4 for each of the four primary reflections. The dotted line is the uncorrected spectrum for reflections including thin beds, while the solid line is the spectrum with no thin beds. The latter spectrum is a close approximation of the actual

Table 1. True and computed values of Q from the synthetic test data, for cases of no thin beds and thin beds added. When thin beds are present, Q values are computed with and without the spectral correction technique.

	True value	No thin beds	Thin beds added (uncorrected)	Thin beds added (corrected)
Q_{LSR} reference to reflection 2	30	32	14	33
Q_{LSR} reference to reflection 3	38	42	14	43
Q_{LSR} reference to reflection 4	29	32	26	29
Q_3 from layer stripping	50	57	15	61
Q_4 from layer stripping	20	22	−38	18

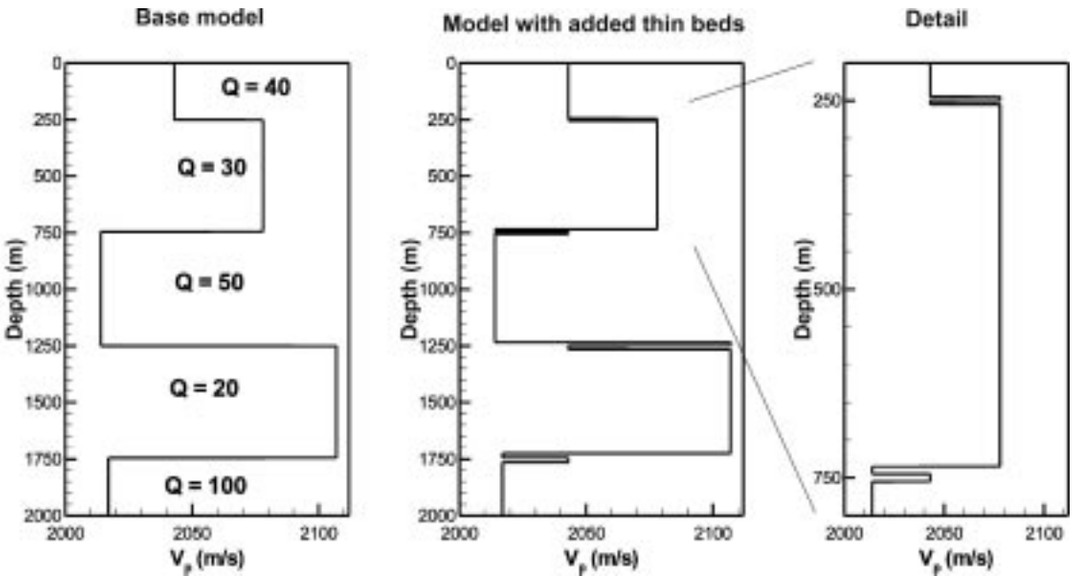

Figure 2. Models for synthetic seismic reflection data without and with thin beds added near each main layer boundary.

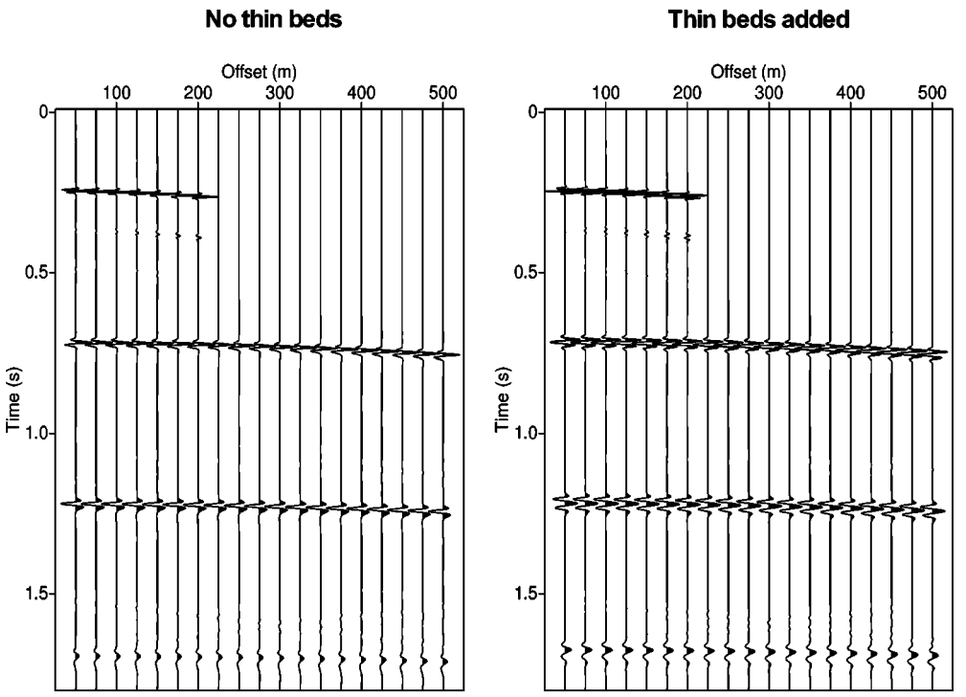

Figure 3. Seismic reflection response of synthetic models without (left) and with (right) thin beds near each main layer boundary. Seismograms are shown with automatic gain control (AGC), since attenuation strongly reduces the amplitude of the later reflections. The low-amplitude reflections following the first reflection are P-S and S-S converted waves. The signals from the first reflector are muted after 200-m offset because of interference from the direct wave.

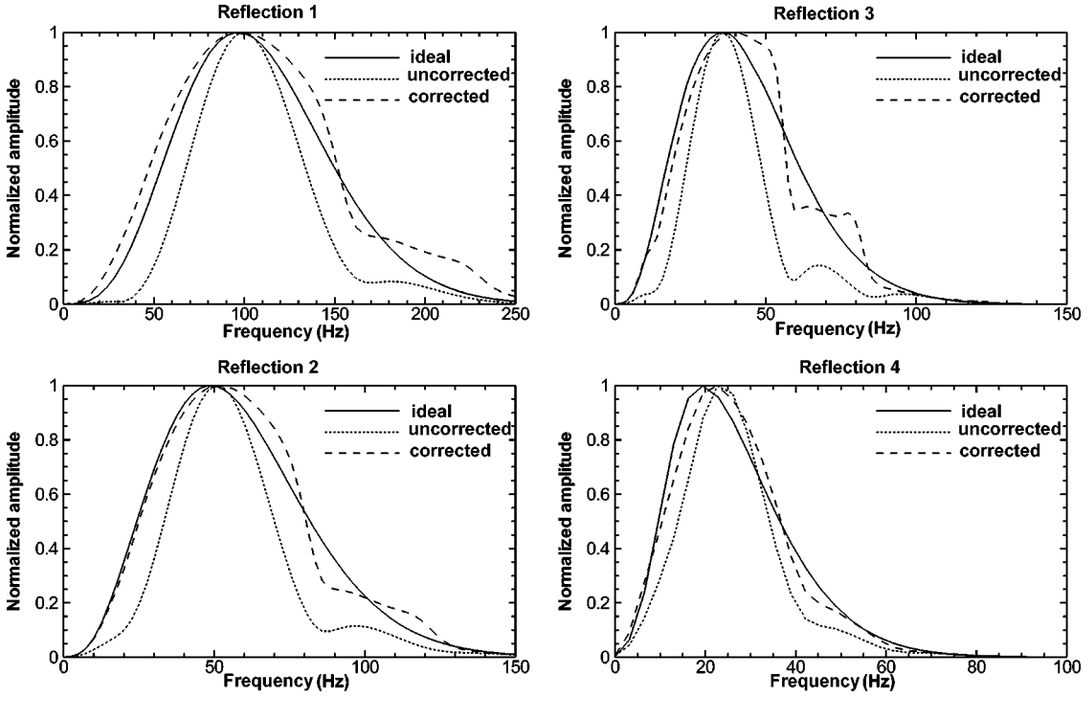

Figure 4. Comparison between uncorrected and corrected normalized local reflection spectra. In each figure, the solid line is the spectrum if there are no thin beds. The dotted line is the spectrum with thin beds present. The dashed line is the corrected spectrum using the well-log deconvolution method. Ideally, the dashed line would coincide with the solid line. The corrected spectrum is, however, a definite improvement over the uncorrected spectrum. Note that not all frequency axes span the same range.

spectrum of the incident wave when thin beds are present; the thin beds introduce complexity in the reflected waveform but, because of the low reflection coefficient, do not significantly impact the transmitted wave. The dashed line is the corrected spectrum for each case. Ideally, the corrected spectrum (dashed line) would exactly match the incident spectrum (solid line). This does not happen because we have imperfectly smoothed out the zeros in the spectrum of the reflectivity stickogram. Nevertheless, the corrected spectrum is an improvement over the uncorrected spectrum, and the differences between corrected and incident spectra appear to average out over a range of frequencies.

The correction method appears to be robust in the presence of moderate amounts of noise and uncertainty. One of the major sources of uncertainty for this technique is the possibility of errors in the well-logs. Errors in the depth-to-time tie between well-log and seismic data are not overly significant, since a shift of a signal in time only affects the phase of the spectrum and not the amplitude. Time shifts may become important if strong reflectors are moved into or out of the time window of the Fourier transform. The use of a tapered windowing function, such as the Hanning window (Oppenheim and Schafer, 1989), can minimize the problem for small time shifts.

Errors in the well-log values are more significant, since they directly alter the reflectivity stickogram used to compute the corrected spectra. To evaluate this effect, we introduced uniform Gaussian noise to the reflectivity stickogram at levels of 1, 2, 5, and 10%, and reprocessed the spectrally corrected Q values for eight realizations of each noise level. The resulting average Q values and their standard deviations are given in Table 2. With increasing well-log error, there is a trend toward increasing uncertainty in Q and a trend toward (in this case) lower Q. The latter follows from equation 6: as the noise level in the reflectivity stickograms increase, the spectra become dominated by the noise, and R_1 and R_2 both approach the noise spectrum. In such a case, R_1 and R_2 cancel out on average, and the mean Q approaches that of the uncorrected spectrum (see Table 1). When the noise added to the reflectivity stickogram reaches 5%, the added error begins to overtake the inherent uncertainty in the calculation, and there is notable deterioration in the accuracy of the spectrally corrected Q factor.

REAL-DATA EXAMPLE

Having successfully demonstrated the correction method in the idealized model data, we now turn to an example using real data. A high-resolution 2D seismic line was acquired over a Florida carbonate aquifer system. (See Parra et al., 2003, for a detailed description of this site.) Figure 5 shows the migrated seismic data and well logs from the site. Since there is little visible lateral variation, we expect the well-log correction technique to be applicable over most of the seismic line. Synthetic seismograms show a good tie between the well log (near

Table 2. Effect of well-log error on uncertainty of computed spectrally corrected Q_{LSR} values. Average values are presented along with the standard deviations derived from eight realizations of each degree of error in the reflectivity stickogram.

	True value	0% error	1% error	2 % error	5% error	10% error
Reference to reflection 2	30	33	33 ± 4	34 ± 8	29 ± 6	16 ± 4
Reference to reflection 3	38	43	43 ± 3	40 ± 6	32 ± 6	26 ± 5
Reference to reflection 4	29	29	30 ± 4	26 ± 5	22 ± 5	24 ± 5

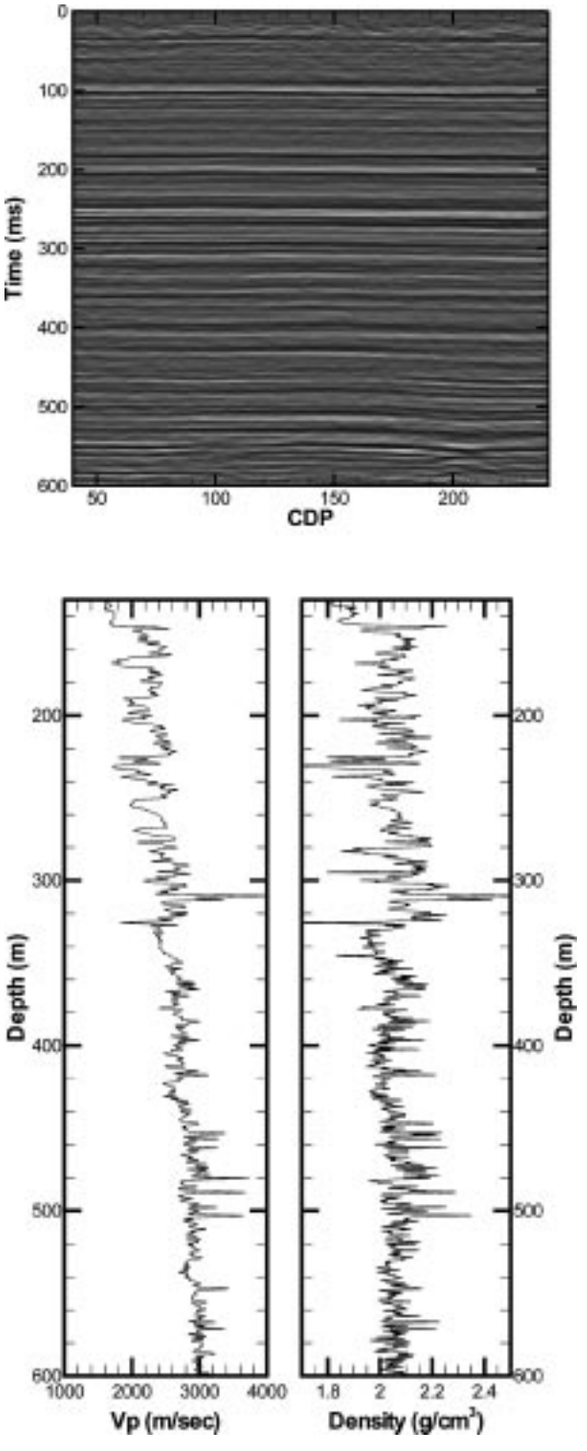

Figure 5. Migrated seismic data and well logs from the Florida test site.

CDP 50) and the actual seismic data. From this data, we take the reference-reflection time window to extend from 0.15 to 0.20 s, and choose two target time windows: 0.30 to 0.36 s and 0.46 to 0.56 s. These times cover roughly the entire range of the well log.

Using the spectral correction technique along with the QVO calculation significantly enhances the stability of the computation of Q. At the top of Figure 6, we show the uncorrected and corrected LSRs as a function of frequency for one five-trace offset stack from a CDP in the middle of the spread, using the reference and first target time windows. Small shifts in the spectral amplitude at a few frequencies make a large difference in the resulting straight-line least-squares fit. The LSR profile using corrected spectra much more closely matches a straight line and produces a rather different (and more realistic) slope. The bottom plots of Figure 6 show the computed Q^{-1} for each offset stack of this CDP. Here, the LSR results are shown as square symbols with error bars, and the CF results are shown as triangles. The spectral corrections not only produce a more consistent value of Q for each offset but also reduce the statistical uncertainty computed from the least-square fit to the LSR profile.

Figure 7 shows the uncorrected (left) and spectrally corrected (right) Q estimates as a function of CDP using both the LSR and CF methods. Here, we plot the average Q^{-1} and the standard deviation within each group of 10 CDPs. The computed Q from the shallower reflection target is highly variable in the uncorrected case, with many negative Q values. After applying the spectral correction, the Q values are much more stable and seem to have an average value of $Q^{-1} \approx 0.03$ ($Q \approx 33$) using the LSR method and $Q^{-1} \approx 0.05$ ($Q \approx 20$) using the CF method. Within the given range of uncertainty, these values hold fairly constant along the length of the line. Apart from a few faults and some small changes in bed thickness, the rock properties at this site are expected to be laterally invariant. For the deeper target reflection, there is not so much change between the uncorrected and corrected Q estimates. The spectrally corrected Q estimate is definitely somewhat improved, however, in terms of fewer negative Q values and slightly less variability. (Negative Q values are physically unrealistic.) Again, we see that $Q^{-1} \approx 0.03$ ($Q \approx 33$) across the length of the line. We would expect the deeper reflection target to produce more stable Q values because of the longer traveltime. In this case, the LSR and CF methods produce generally similar results, which gives us additional confidence in the computed Q values.

CONCLUSIONS

Reflected wavelets can be altered in the time and frequency domains by the presence of thin beds near the primary reflector. These changes make it more difficult to extract reliable Q information from the seismic data. We have demonstrated the successful use of a well-log–based spectral correction method for improving Q estimation with QVO analysis of surface seismic data. In this method, the spectrum of the reflection is divided

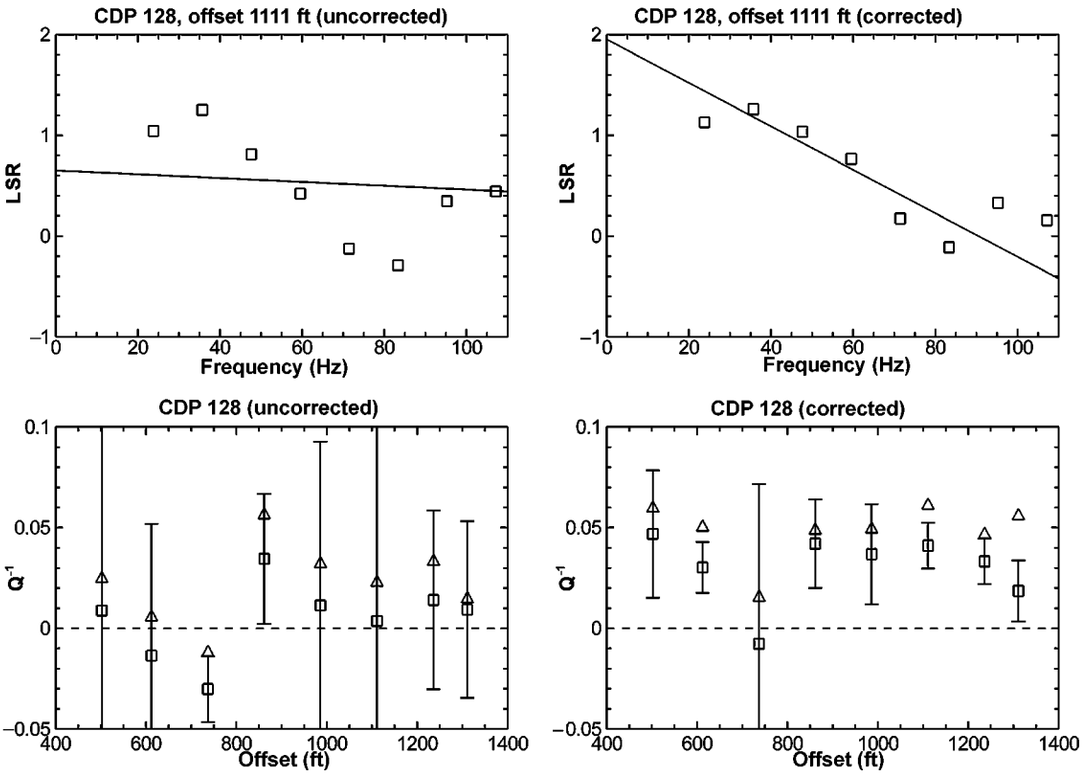

Figure 6. (top) Plots of corrected and uncorrected log-spectral ratio (LSR) as a function of frequency for CDP 128, offset 1111 ft, in the Florida data. (bottom) Q^{-1} versus offset plots for CDP 128 of LSR Q^{-1} (square symbols with error bars) and centroid-frequency (CF) Q^{-1} (triangles). This data uses the 0.18 s and 0.34 s window centers.

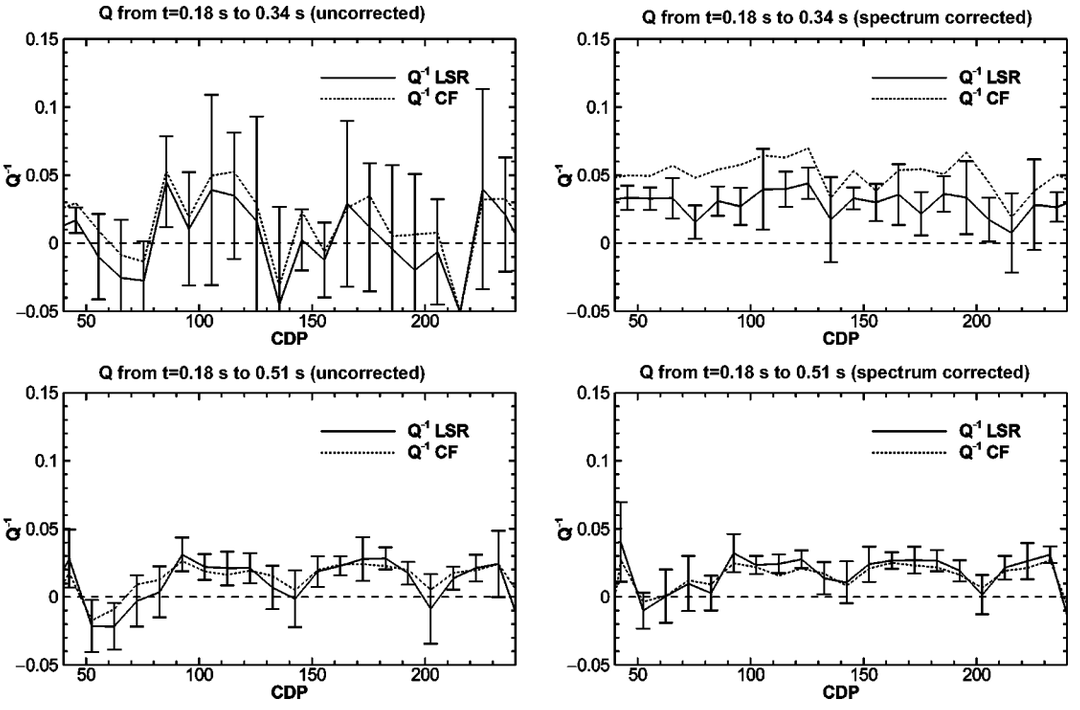

Figure 7. Comparison of uncorrected (left) and corrected (right) Q^{-1} values computed from two sets of reflections from the Florida seismic line. Plotted are the average and standard deviation of Q^{-1} over groups of 10 CDP using both the LSR and CF methods. The corrected values have less variance and fewer negative Q values.

by the spectrum of the local reflectivity stickogram before Q is computed. An inherent assumption is that the observed reflections consist of primaries only (multiple-free). We test the method using synthetic seismograms, and then apply it to real data. The Q values computed using the corrected spectra have less variance and fewer negative values than those computed with uncorrected spectra. We find an average Q value near 33 for sediments from roughly 170- to 600-m depth at the south Florida test site. This value generally holds stable along the length of the seismic line using both LSR and CF methods for Q extraction.

The success of this method depends on a good local tie from the well log to the seismic data. The need for time windows to bracket each reflection group means that Q inversion will be a low-resolution process. The time windows must be long enough (i.e., several periods of the peak frequency of the waveform) so that a Fourier transform produces several frequencies within the bandwidth of the pulse. Otherwise, there will be too few data points for the LSR or CF methods to be reliable. Furthermore, for accurate estimation of traveltimes, the separation between time windows must be several times their length. For most cases, then, the recovered Q estimates will be averages over a hundred meters or more of depth. Nevertheless, in many formations, this may be sufficient to find evidence of gas, fractures, or change in lithology. If many overlapping Q measurements are taken, there is also the possibility of downscaling the low-resolution Q information to a higher resolution in conjunction with seismic or borehole data.

ACKNOWLEDGMENTS

This manuscript was greatly improved by the comments of the anonymous reviewers. We wish to thank Michael Bennett and the South Florida Water Management District for access to data and the site. Bay Geophysical acquired the seismic data. This paper was prepared with the support of the U.S. Department of Energy under Award No. DE-FC26-02NT15343. However, any opinions, findings, conclusions, or recommendations expressed herein are those of the authors and do not necessarily reflect the views of the DOE. Thanks also to Purna Halder (DOE) for his support of this work.

REFERENCES

Dasgupta, R., and R. A. Clark, 1998, Estimation of Q from surface seismic reflection data: Geophysics, **63**, 2120–2128.
Ganley, D. C., and E. R. Kanasewich, 1980, Measurement of absorption and dispersion from check shot surveys: Journal of Geophysical Research, **85**, 5219–5226.
Hauge, P. S., 1981, Measurements of attenuation from vertical seismic profiles: Geophysics, **46**, 1548–1558.
Higdon, R. L., 1991, Absorbing boundary conditions for elastic waves: Geophysics, **56**, 231–241.
Korneev, V. A., G. M. Goloshubin, T. M. Daley, and D. B. Silin, 2004, Seismic low-frequency effects in monitoring fluid-saturated reservoirs: Geophysics, **69**, 522–532.
Neep, J. P., M. S. Sams, M. H. Worthington, and K. A. O'Hara-Dhand, 1996, Measurement of seismic attenuation from high-resolution crosshole data: Geophysics, **61**, 1175–1188.
O'Doherty, R. F., and N. A. Anstey, 1971, Reflections on amplitudes: Geophysical Prospecting, **19**, 430–458.
Oppenheim, A. V., and R. W. Schafer, 1989, Discrete-time signal processing: Prentice Hall.

Parra, J. O., and C. L. Hackert, 2002, Wave attenuation attributes as flow unit indicators: The Leading Edge, **21**, 564–572.
Parra, J. O., C. Hackert, M. Bennett, and H. A. Collier, 2003, Permeability and porosity images based on NMR, sonic, and seismic reflectivity: Application to a carbonate aquifer: The Leading Edge, **22**, 1102–1108.
Pride, S., et al., 2003, Permeability dependence of seismic amplitudes: The Leading Edge, **22**, 518–525.
Quan, Y., and J. M. Harris, 1995, Seismic attenuation tomography using the frequency shift method: Geophysics, **62**, 895–905.
Raikes, S. A., and R. E. White, 1984, Measurements of earth attenuation from downhole and surface seismic recordings: Geophysical Prospecting, **32**, 892–919.
Rapoport, M. B., L. I. Rapoport, and V. I. Ryjkov, 2004, Direct detection of oil and gas fields based on seismic inelasticity effect: The Leading Edge, **23**, 276–278.
Robertson, J. D., and H. H. Nogami, 1984, Complex seismic trace analysis of thin beds: Geophysics, **49**, 344–352.
Sheriff, R. E., and L. P. Geldart, 1995, Exploration seismology, 2nd ed.: Cambridge University Press.
Sun, X., X. Tang, C. H. Cheng, and L. N. Frazer, 2000, P- and S-wave attenuation logs from monopole sonic data: Geophysics, **65**, 755–765.
White, R. E., 1992, The accuracy of estimating *Q* from seismic data: Geophysics, **57**, 1508–1511.
Zhang, C., and T. J. Ulrych, 2002, Estimation of quality factors from CMP records: Geophysics, **67**, 1542–1547.